Received: 13 November 2018 | Revised: 24 January 2019 | Accepted: 13 February 2019

DOI: 10.1111/jace.16386

ORIGINAL ARTICLE

Journal of the American Ceramic Society

Enhanced spontaneous polarization in double perovskite Bi_2FeCrO_6 films

Dehuan Meng[1] | **Yunsheng Xiao**[1] | **Hongcai He**[1] | **Yulong Liao**[1] | **Huaiwu Zhang**[1] | **Junyi Zhai**[2,3] | **Zuhuang Chen**[4,5] | **Lane W. Martin**[4,5] | **Feiming Bai**[1]

[1]State Key Laboratory of Electronic Thin films and Integrated Devices, University of Electronic Science and Technology, Chengdu, China

[2]CAS Center for Excellence in Nanoscience, Beijing Key Laboratory of Micro-nano Energy and Sensor, Beijing Institute of Nanoenergy and Nanosystems, Chinese Academy of Science, Beijing, China

[3]College of Nanoscience and Technology, University of Chinese Academy of Sciences, Beijing, China

[4]Department of Materials Science and Engineering, University of California, Berkeley, California

[5]Materials Sciences Division, Lawrence Berkeley National Laboratory, Berkeley, California

Correspondence
Feiming Bai, State Key Laboratory of Electronic Thin films and Integrated Devices, University of Electronic Science and Technology, Chengdu, China.
Email: fmbai@uestc.edu.cn
and
Junyi Zhai, CAS Center for Excellence in Nanoscience, Beijing Key Laboratory of Micro-nano Energy and Sensor, Beijing Institute of Nanoenergy and Nanosystems, Chinese Academy of Science, Beijing, China.
Email: jyzhai@binn.cas.cn

Funding information
National Science Foundation, Grant/Award Number: DMR-1708615; National Key Research and Development Plan, Grant/Award Number: 2016YFA0300801; 2017YFB0406400; National Science Foundation of China, Grant/Award Number: 61871081,

Abstract

We report the pulsed-laser deposition of epitaxial double-perovskite Bi_2FeCrO_6 (BFCO) films on the (001)-, (110), and (111)-oriented single-crystal $SrTiO_3$ substrates. All of the BFCO films with various orientations show the $^1/_2{}^1/_2{}^1/_2$ and $^3/_2{}^3/_2{}^3/_2$ superlattice-diffraction peaks. The intensity ratios between the $^1/_2{}^1/_2{}^1/_2$-superlattice and the main 111-diffraction peak can be tailored by simply adjusting the laser repetition rate and substrate temperature, reaching up to 4.4%. However, both optical absorption spectra and magnetic measurements evidence that the strong superlattice peaks are not correlated with the *B*-site Fe^{3+}/Cr^{3+} cation ordering. Instead, the epitaxial (111)-oriented Bi_2FeCrO_6 films show an enhanced remanent polarization of 92 μC/cm^2 at 10 K, much larger than the predicted values by density-functional theory calculations. Positive-up-negative-down (PUND) measurements with a time interval of 10 μs further support these observations. Therefore, our experimental results reveal that the strong superlattice peaks may come from *A*- or *B*-site cation shifts along the pseudo-cubic [111] direction, which further enhance the ferroelectric polarization of the BFCO thin films.

KEYWORDS

anomalous photovoltaic, bandgap, ferroelectric materials, magnetization, perovskite oxides

1 | INTRODUCTION

Sunlight is one of the most abundant resources to generate renewable energy. Researchers are continuously exploring new materials and fundamental photoelectric conversion mechanisms for the better performance of photovoltaic (PV) devices.[1–3] Of particular interests is the anomalous photovoltaic effect in ferroelectric (FE) materials, characterized by large open circuit photovoltages exceeding the band gap of the material.[4–6] In addition, the photocurrent can be switched by presetting the polarization direction.[7–9] However, the wide bandgap (E_g) of typical perovskite FE materials exceeds the ideal value of 1.4-2.1 eV, making them unsuitable for absorbing sunlight. This wide E_g is mainly due to the transition metal–oxygen bonds at *B* sites and the large difference in their electronegativities.[10] Even $BiFeO_3$ (BFO) with a narrow bandgap of 2.74 eV is only capable of absorbing 20% of the solar spectrum, prompting the exploration of novel FE materials.

Lowering the E_g while maintaining FE properties is a promising route to boost power conversion efficiency. So far, efforts have been taken to synthesis $LaCoO_3$-doped $Bi_4Ti_3O_{12}$,[11] $KBiFe_2O_5$,[12] and $[KNbO3]_{1-x}[BaNi_{1/}2Nb_{1/2}O_{3-\delta}]_x$[10] (KBNNO) solid solutions, etc. The non-perovskite $KBiFe_2O_5$ has an E_g of 1.6 eV, and an ideal E_g of 1.39 eV was achieved in KBNNO for x = 0.1. However, these materials have poor remanent polarization, degrading the benefits of anomalous photovoltaic effects. One exception is the double perovskite Bi_2FeCrO_6 (BFCO). Density-functional theory calculations by different authors have predicted the coexistence of a large remanent polarization (P_r) of 80 μC/cm^2 along the [111] at 0 K and a narrow E_g of 1.4-2.0 eV.[13,14] Unfortunately, the synthesis of BFCO has been hindered by a lack of stability of the bulk Bi-based perovskites and disordered Fe^{3+} and Cr^{3+} on the *B* sites,[15] due to the same valence state and very close ionic radii. Highly ordered BFCO films were first reported in a superlattice form prepared by alternating deposition of $BiFeO_3$ and $BiCrO_3$ layers.[16] Later, partially ordered BFCO was also reported by several research groups using pulsed-laser deposition from a single $BiFe_{0.5}Cr_{0.5}O_3$ target.[17,18] The degree of *B*-site ordering was monitored by the intensity ratio (*R*) between the $^1/_2{}^1/_2{}^1/_2$-superlattice and 111-diffraction conditions,[19] which typically ranges from 0%-5.1%. It was reported that the bandgap of the BFCO films is strongly correlated with the *B*-site cation ordering, and E_g varies between 1.4 and 2.6 eV as the *R* value decreases.[19] However, given the low X-ray scattering contrast between the Fe^{3+} and Cr^{3+}, it was recently argued that the observation of a superstructure is not a sufficient proof of *B*-site ordering in double perovskites,[20,21] and in fact the truly *B*-site ordered double perovskite has relatively lower R value less than 1%, for example La_2FeCrO_6 film deposited on (111)-oriented STO substrate.[22]

Here, we report the preparation of epitaxial BFCO films on single-crystal $SrTiO_3$ substrates by pulsed-laser deposition. Efforts have been taken to investigate the critical processing window to obtain superlattice peaks. The origin of the superlattice peaks and the relationships between the R ratio and the *B*-site cation ordering have been examined by performing combined optical, magnetic, and ferroelectric analysis. Our experimental results suggest that the superlattice peaks may originate from the displacements of *A*- or *B*-site cations along the [111], which can enhance the ferroelectric polarization of BFCO films.

2 | EXPERIMENTAL

A ceramic target with a nominal composition of $Bi_{1.1}Fe_{0.5}Cr_{0.5}O_3$ was synthesized by the conventional solid-state reaction method. Bi_2O_3, Fe_2O_3, Cr_2O_3 powder were mixed together with molar ratios 2.2:1:1, where the excess of Bi compensates the loss due to its volatility at high temperatures. The powder mixture pellet was then heated at 830°C for 60 minutes, then the sample was cooled to room temperature slowly. Bi_2FeCrO_6 thin films were grown on (001)-, (110)-, (111)-oriented $SrTiO_3$ (STO) single-crystal substrates by pulsed-laser deposition with a KrF excimer laser (λ = 248 nm). 50-nm-thick $SrRuO_3$ (SRO) films, used as a bottom electrode for ferroelectric property study, were deposited at a heater temperature of 660°C in a dynamic oxygen pressure of 100 mTorr with a laser energy density of 1.5 J/cm^2 and a laser repetition of 5 Hz. The BFCO films were deposited at the heater temperature between 650°C and 750°C, in a dynamic oxygen pressure of 9 mTorr, with a laser energy density of 1.5 J/cm^2 and a laser repetition ranging from 2 to 12 Hz from a target of composition $Bi_{1.1}(Fe_{0.5}Cr_{0.5})O_3$. The thickness of the BFCO films was fixed to be 300 nm. After depositions, the films were cooled to 400°C at a rate of 5°C/min and annealed for 1 hour in 760 Torr oxygen and then slowly cooled to room temperature. To perform polarization measurements, Au top electrodes were sputtered through a shadow mask of 100 μm in diameter.

The structure of the BFCO films was probed using high-resolution X-ray diffraction (Bruker, D8 discover). The Energy Dispersive X-Ray Spectroscopy (EDX) of the BFCO thin films were measured using a Scanning Electron Microscope equipped with IXRF system (SU8020, Hitachi). The magnetic properties were measured at temperatures ranging from 4.2-300 K using a physical property measurement system (PPMS, Quantum Design). The transmittance of the BFCO films, deposited on double-polished STO substrates, was measured via a UV-VIS-NIR Spectrometer (UV-3600, Shimadzu Co.). Ferroelectric hysteresis loops (P-E loops) and positive-up-negative-down (PUND) measurements were

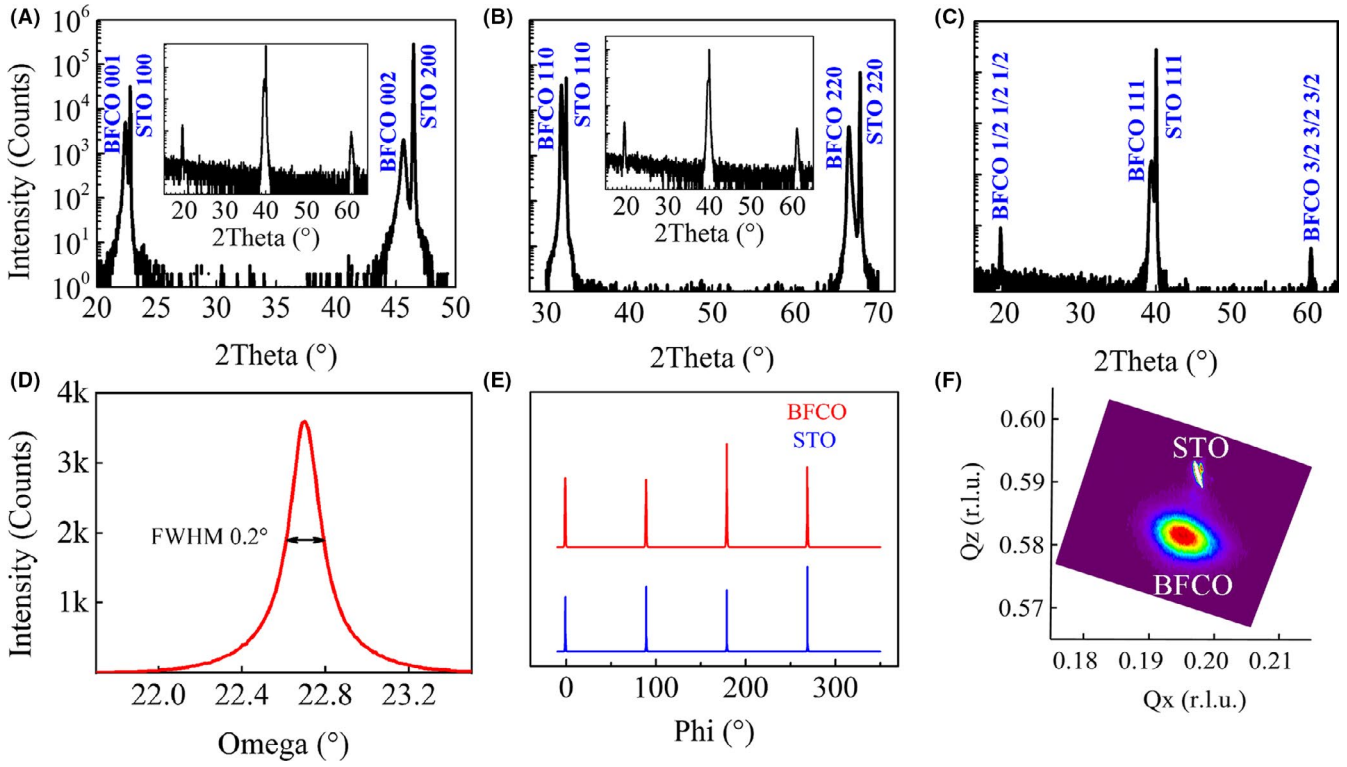

FIGURE 1 XRD θ-2θ scans of BFCO films deposited on (A) the (001)-, (b) (110)- and (c) (111)-oriented STO substrates. The inserts of Figure 1A,B show the measured *hhh*-diffractions peaks of the BFCO films deposited on the (001)- and (110)-oriented STO substrates. D, The rocking curve of (002) peak corresponding to the (001)-oriented film. E, Phi-scans about the 202-diffraction peaks of the (001)-oriented BFCO films. F, Reciprocal space mapping about 103-diffraction peak of the (001)-oriented BFCO film [Colour figure can be viewed at wileyonlinelibrary.com]

performed using a ferroelectric tester (Precision Multiferroic, Radiant Technologies).

3 | RESULTS AND DISCUSSION

3.1 | Crystal structure of BFCO thin films

The *R*3 symmetry of the double perovskite BFCO can be approximated with a pseudo-cubic one. Figure 1A-C show the XRD θ-2θ scans of the (001)-, (110)-, and (111)- oriented BFCO films grown at 720°C with a laser repetition of 6 Hz. All films are highly oriented with only pseudo-cubic 00*l*-, *h*0*h*-, and *hhh*-diffraction peaks, in addition to the STO substrate peaks. Rocking curve studies of the 002-diffraction peak of the (001)-oriented BFCO film reveals the good crystal quality of the heterostructures (Figure 1D). Phi-scans about the 202-diffraction peaks (Figure 1E) and reciprocal space mapping studies (Figure 1F) about the 103-diffraction peak of the (001)-oriented BFCO films show that the BFCO films are fully epitaxial along both the in-plane and out-of-plane directions. The out-of-plane lattice parameter is 3.974 Å and the in-plane lattice parameter is 3.945 Å, indicating that the strain between the epitaxial BFCO thin film and the STO substrate is partially relaxed. The calculated cell volume of BFCO is 61.847 Å^3, which is larger than the value reported in the literature.[19] For the (111)-oriented BFCO films, superlattice $^1/_2{}^1/_2{}^1/_2$- and $^3/_2{}^3/_2{}^3/_2$-diffraction peaks at 19.45° and 60.71°, respectively are observed (Figure 1C). The calculated intensity ratio $I_{½\,½\,½}/I_{111}$ is 4.4%, close to that of what has been reported for highly ordered BFCO (5.1%).[19] We have also measured the *hhh*-diffractions peaks of the BFCO films deposited on the (001)- and (110)-oriented STO substrates (The inserts of Figure 1A,B). Both films exhibited strong superlattice peaks with $R > 3\%$.

The relationships between the R ratio, the substrate temperature, and the laser-repetition rate were further plotted (Figure 2A). R values above 1% were obtained in the BFCO films deposited at temperatures ranging from 675 to 725°C with a laser-repetition rate ranging from 2 to 8 Hz. High substrate temperature and low repetition rate (or growth rate) are beneficial to obtain high *R* values.[19] Figure 2B shows the dependence of the lateral correlation length (*D*) on the substrate temperature and the laser-repetition rate. *D* was calculated from the linewidth of the $^1/_2{}^1/_2{}^1/_2$-superlattice peak, which was previously interpreted as the ordered domain size.[19,20] Clearly, large $D > 40$ nm can be obtained with high substrate temperature and low repetition rate. The highest *R* of 4.4% and the largest *D* of 60 nm were obtained

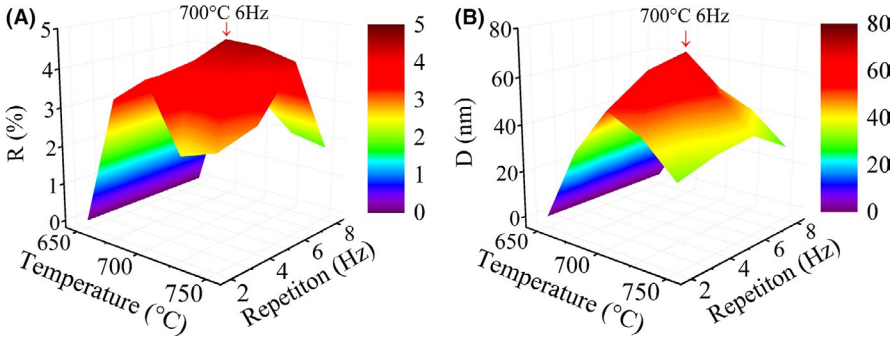

FIGURE 2 Dependence of (A) R ratio and (B) lateral correlation length (D) on the substrate temperature and laser repetition rate [Colour figure can be viewed at wileyonlinelibrary.com]

in the BFCO films deposited at 720°C with a laser repetition of 6 Hz, as already shown in Figure 1. It is realized that changing the substrate temperature or repetition rate may vary the chemical composition of the resulting films, so we have also analyzed the chemical compositions of BFCO films with different *R* values, as shown in Figure S1. The determined chemical compositions are $Bi_{2.04}Fe_{1.04}CrO_{6.12}$, $Bi_{2.0}Fe_{1.04}CrO_{6.06}$ and $Bi_{1.98}Fe_{1.04}CrO_{6.03}$, respectively. Although the Bi content decreases with increasing the substrate temperature and lowering repetition rate, it is important to notice that the Fe/Cr ratio remains the same for all the BFCO films with $R = 0$, 1.9%, and 4.4%. It is known that the A-site ion has very important influence on the superstructure of perovskite oxides. A-site vacancies and doping have been widely used to improve B-site order of double-perovskite materials.[23–25] It was suggested that a smaller A-site ion size favors long-range B-site ordering. Additionally, the large polarizability of the bismuth ion may also influence ordering in Bi-based perovskite systems. So the BFCO film with lower Bi content exhibited enhanced R value. However, the detailed mechanism is still under investigation.

The stacking ordering of $BiFeO_3$ and $BiCrO_3$ and the spin configuration could heavily influence the electronic properties of BFCO. For instance, Baettig *et al* have predicted that the ground-state structure of BFCO is *insulating* with *R*3 symmetry and exhibits simultaneously ferroelectric and *ferromagnetic* order.[13,26] However, Song and Liu predicted a robust *ferrimagnetic semiconducting* phase with a narrow bandgap (E_g) of 1.4-1.7 eV due to crystal-field and spin-exchange splitting.[14] Later, Goffinet *et al* suggested that BFCO presents two competing *ferrimagnetic* phases, sharing the same total magnetic moment but with a different electronic configuration for the Fe^{3+} species.[27] Clearly, there are quite a few discrepancies as to the bandgap of BFCO. In essence, it is important to better understand (i) what the intrinsic bandgap of BFCO is and (ii) whether the large R ratios come from Fe/Cr cation ordering or not. In order to address these questions,

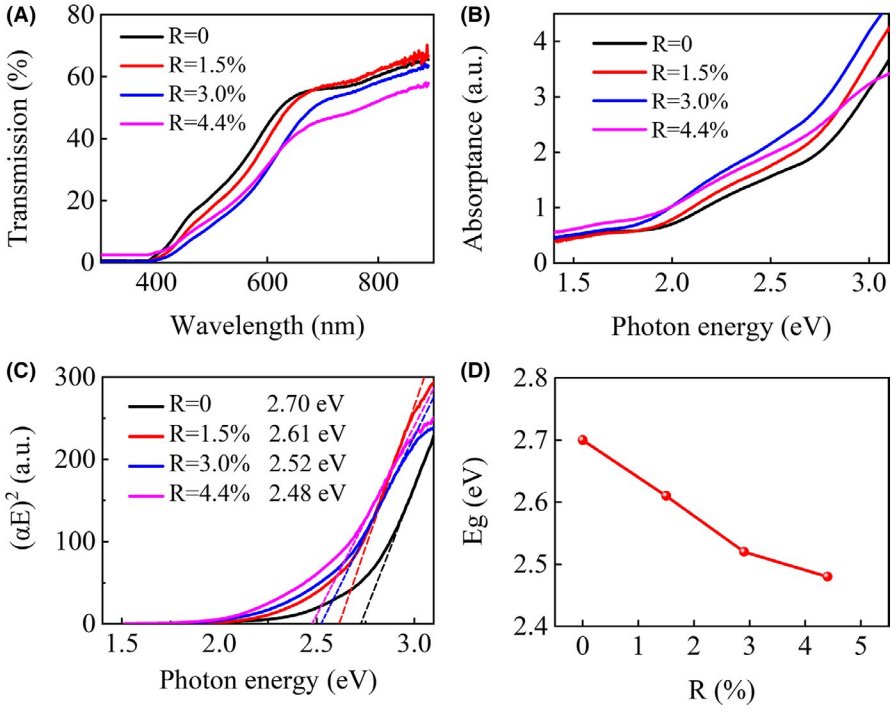

FIGURE 3 The (A) transmission and (B) absorption spectra of the (111) BFCO thin films with different intensity ratio. C, The plots of photon energy $h\nu$ vs $(\alpha h\nu)^2$ for bandgap determination. D, The relationship between the bandgap and R ratio for the (111) BFCO thin films [Colour figure can be viewed at wileyonlinelibrary.com]

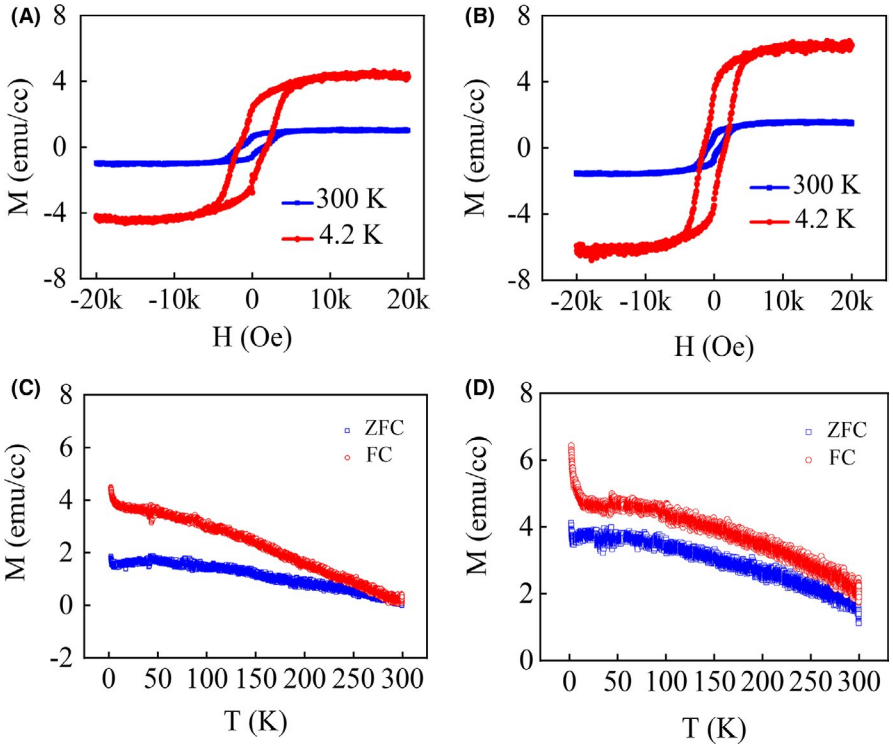

FIGURE 4 The magnetic hysteresis loops of the (111)-oriented BFCO thin films with (A) R = 0% and (B) R = 4.4% measured at 300 K and 4.2 K, respectively. Temperature-dependent magnetization of the (111)-oriented BFCO films with (C) R = 0% and (D) R = 4.4% [Colour figure can be viewed at wileyonlinelibrary.com]

the bandgap and magnetic properties of the BFCO thin films were characterized and analyzed in the following.

3.2 | Bandgap of BFCO thin films

Figure 3A,B are the transmission and absorption spectra of the (111)-oriented BFCO films with different *R* ratios deposited on double-polished STO substrates. Using the photon energy hv vs $(\alpha hv)^2$ plot (where α is the absorption coefficient), we were able to extrapolate the direct bandgap of BFCO film (Figure 3C). The direct bandgap of the samples slightly decreased from 2.7 to 2.48 eV when the *R* ratio increases from 0 to 4.4% (Figure 3D). Figure S2 further shows the direct bandgap of the (001)-, (110)-, and (111)-oriented samples with $R = 4.4\%$, which varied slightly from 2.48 to 2.52 eV depending on the volume fraction of stressed BFCO on the STO substrates. It is known that oxygen vacancies and point defects may introduce sub-band gap levels and affect optical properties.[28,29] This is the reason causing the presence of a shoulder or distinct satellite peaks on the absorption spectra on the low bandgap side.[19,30] Since we have not observed these features in Figure 3C, we believe that the influence of point defects on optical properties is low and the red shift of absorption can be attributed to the appearance of the superlattice structure. However, please notice the corresponding correlation length of the sample is about 60 nm. Clearly, even the presence of strong superlattice peaks and large correlation lengths cannot pull down the bandgap of BFCO films below 2 eV, which was believed to the intrinsic E_g of *B*-site cation ordered BFCO.[14,19]

3.3 | Magnetic properties of BFCO thin films

On account of the magnetic moments of Fe^{3+} (5 μB) and Cr^{3+} (3 μB), antiferromagnetic *B*-site ordered arrangement leads to a net magnetic value of 2 μB per formula unit, corresponding to ~160.5 emu/cm^3.[13] For partially ordered BFCO, the relationship between saturation magnetization and Fe/Cr ordering can be described by the equation: $M_s = (2\text{-}4AS)$ μB/fu (where AS refers to antisite defects).[22] So, the M_s of completely ordered BFCO thin films will be 2 μB/fu and that of the completely disordered phase should be zero. Figure 4A,B compare the magnetization versus field curves for two BFCO thin films deposited on (111)-oriented STO substrates with $R = 0$ and $R = 4.4\%$. At 4.2 K, the measured saturation magnetization values are 4.5 emu/cc (0.056 μB/fu) and 6.2 emu/cc (0.078 μB/fu), respectively. The measured saturation magnetization did not increase much with the *R* ratio increasing from 0 to 4.4%, and is much smaller than the expected value (2 μB/fu), indicating a potential lack of *B*-site Fe/Cr cation ordering. The low magnetic moment may come from a small degree of Cr^{3+}-Fe^{3+} ferromagnetic exchange or magnetic nanoclusters. Although the coercive magnetic field is high, it maybe correlated with the size and distribution of these magnetic nanoclusters. In addition, structural defects may pin these magnetic nanocluster and contribute the extrinsic high coercive field. Figure 4C,D show the field-cooled and zero-field-cooled magnetization curves measured in the temperature range 4.2-300 K. Unlike recent finding of spin glass state in B-site ordered Bi_2FeMnO_6 films,[31] our measurements

of FC and ZFC magnetization curves show a minor magnetization with no evidence of a magnetic transition. Therefore, the magnetism appears to be dominated by antiferromagnetic d^3-d^3 (Cr^{3+}-Cr^{3+}) and d^5-d^5 (Fe^{3+}-Fe^{3+}) coupling. Our absorption analysis together with magnetization results suggest that the presence of the superlattice $^1/_2{}^1/_2{}^1/_2$- and $^3/_2{}^3/_2{}^3/_2$-diffraction peaks alone is not a sufficient proof of Fe^{3+}/Cr^{3+} ordering.

3.4 | Ferroelectric response in BFCO thin films

In perovskite materials, superlattice peaks can arise not only due to cation ordering but also because of *A*- or *B*-site cation shifts and tilts of the oxygen octahedra.[21] Among these, the oxygen octahedra distortions may come from different symmetry between the substrate and the film or lattice mismatch. However, for the current 300-nm-thick BFCO/STO system, the oxygen octahedral distortions can only play a trivial role, if any. So the strong superlattice peaks may be rooted in the displacements of the Bi^{3+}, Fe^{3+}, and Cr^{3+} cations along the [111], as suggested by Shabadi and coauthors.[21] It should also be noted that such cation displacements could generally influence the polarization and ferroelectricity of perovskite thin films.[32–35]

In order to investigate the relationship between the superlattice peaks and the ferroelectricity of BFCO thin films, the polarization-electric field (*P-E*) hysteresis loops of the (100)-, (110)-, and (111)-oriented BFCO films were probed at 10 K (Figure 5A-C). All measurements were carried out at a fixed ac frequency of 2 kHz. Surprisingly, the BFCO thin films with high R ratio (4.4%) show very large spontaneous polarization. The measured spontaneous polarization values were 52, 75, 92 μC/cm^2 for the (001)-, (110)-, and (111)-orientated BFCO films, respectively. The coercive field was about 600 kV/cm, which is larger than the value of BFO films.[36] Figure 5A-C also show the leakage current loops of the (001)-, (110)-, and (111)-oriented BFCO films measured at 10 K. The true remanent polarization can be further calculated from the *P-E* loops after subtracting the leakage-current contribution (Figure 5D-F). For the (001)-oriented BFCO films (Figure 5D), the measured *P*r at 10 K was 50 μC/cm^2 and higher *P*r values were obtained in the (110)- and (111)-oriented films, 73 and

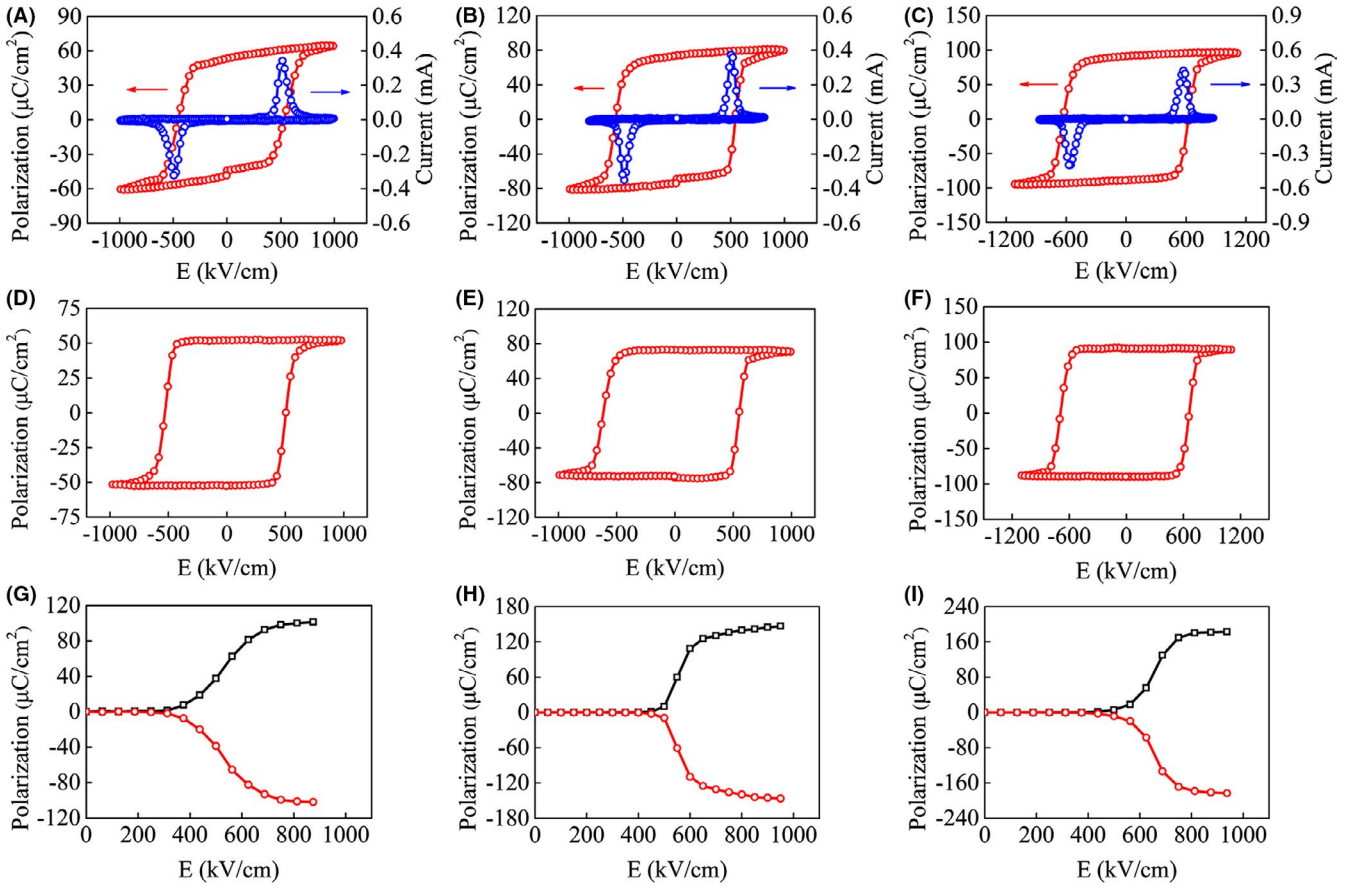

FIGURE 5 A-C, *P-E* curves and leakage current loops of the (001)-, (110)-, and (111)-oriented BFCO films measured at 10 K. D-F, *P-E* loops of the (001)-, (110)-, and (111)-oriented BFCO films after subtracting the contribution from leakage current. G-I, Remanent polarization (2Pr) of the (001)-, (110)-, and (111)-oriented BFCO films as a function of applied electrical field from PUND measurements at 10 K with a time interval of 10 μs [Colour figure can be viewed at wileyonlinelibrary.com]

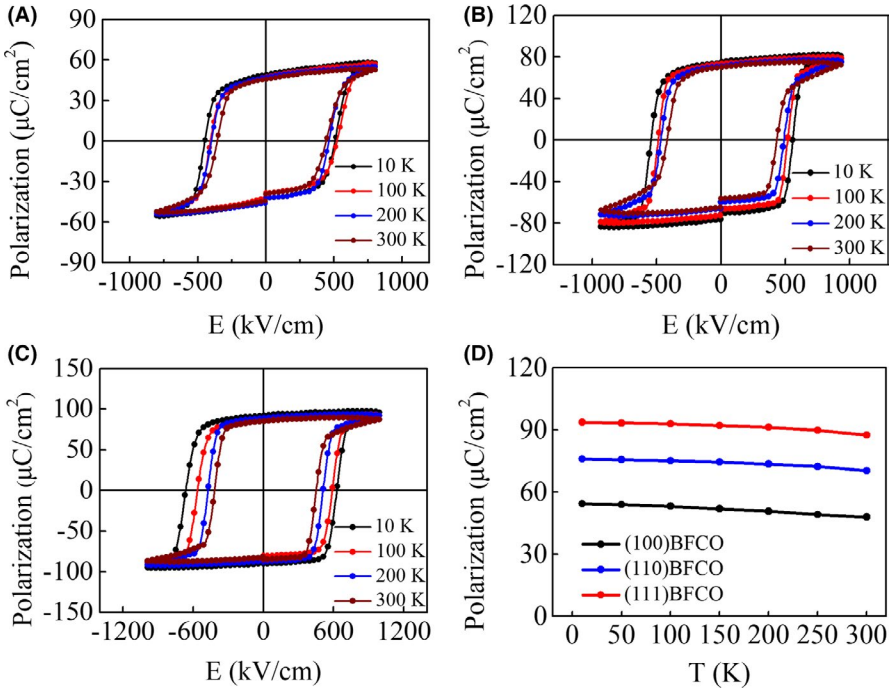

FIGURE 6 The polarization-electric field (*P-E*) hysteresis loops of the (A) (100)-, (B) (110)-, and (C) (111)-oriented BFCO films at various temperature; Temperature-dependent remanent polarization of the BFCO films (D) [Colour figure can be viewed at wileyonlinelibrary.com]

91 μC/cm^2, respectively, at 10 K (Figure 5E,F). Our measurements confirm that the spontaneous polarization direction of BFCO films lies close to the [111], which is similar with $BiFeO_3$.[37] However, the BFCO thin films with low R ratio (1.9%) show relatively low spontaneous polarization. The measured spontaneous polarization values were 45, 62, 80 μC/cm^2 for the (001)-, (110)-, and (111)-orientated BFCO films with $R = 1.9\%$, respectively (Figure S3). Compared to the polarization of BFCO films with low *R* ratio (1.9%), the spontaneous polarization values of BFCO films with high R ratio (4.4%) were enhanced about 15%.

In order to obtain the intrinsic ferroelectric properties, we then performed positive-up negative-down (PUND) measurements using a minor time interval of 10 μs, sufficient to separate the contribution from leakage current and paraelectric effects. Figure 5G-I show the remanent polarization from PUND measurements as a function of applied electrical field at 10 K. Upon increasing the applied electrical field, more ferroelectric domains became switchable, therefore contributing to the enhanced $2P_r$. $2P_r$ for all the tested films almost saturated at 900 kV/cm. The measured $2P_r$ values at 900 kV/cm for the (001)-, (110)-, and (111)-oriented BFCO films are 100, 147, and 183 μC/cm^2, respectively, consistent with those from the *P-E* measurements (Figure 5D-F). Figure 6 shows temperature-dependent remanent polarization of the (001)-, (110)-, and (111)-oriented BFCO films, demonstrating slow decrease of FE polarization with temperature. Therefore, a high Curie temperature is expected.

It should be noted that the measured polarization is much larger than that calculated from the Berry phase in Refs. [13] and [26]. Such a difference may be attributed to fact that (i) the real lattice parameters and unit-cell volume in the current work are larger than those in calculation,[13,26] and (ii) there are potentially additional displacements of Bi^{3+}, Fe^{3+}, and Cr^{3+} cations along the [111]. In fact, previous Rietveld refinement of powder neutron diffraction data showed that the Bi and mixed *B* site Fe/Cr cations are displaced from their ideal positions along the pseudocubic [111] (threefold symmetric [001] hexagonal direction) by 0.58 and 0.22 Å, respectively.[15] Taking the effective charges in ground-state *R*3*c* Bi_2FeCrO_6 of 4.4, 3.5, and −2.5 for Bi, Fe, and O, respectively,[26] the spontaneous polarization can be estimated by summing up formal charges times displacements for all ions in the unit cell, which yields ~83.3 μC/cm^2. Additionally, considering the displacements of Bi^{3+}, Fe^{3+}, and Cr^{3+} cations along the [111], the polarization of (111)-oriented BFCO film can reach up to 92 μC/cm^2.

4 | CONCLUSIONS

In summary, (001)-, (110)-, and (111)-oriented epitaxial BFCO films were grown on $SrTiO_3$ substrates by a pulsed-laser deposition. We report the achievement of both enhanced Pr and low Eg of ~2.5eV in various oriented BFCO film with distinct superlattice peaks. However, according to magnetization measurements of the BFCO thin films, the possibility that the observed strong superlattice peaks come from Fe/Cr cation order is excluded. This observation is further supported by bandgap analysis. We believe that the cation displacements along the [111] give rise to the strong superlattice peaks and enhance the ferroelectric polarization of the

BFCO films. High spontaneous polarization of ~92 μC/cm^2 was measured for the (111)-oriented BFCO films at 10 K. Our findings open a new pathway to regulate the ferroelectric properties of BFCO thin film, and offer new avenues for exploiting properties and applications of double perovskite materials.

ACKNOWLEDGMENT

The authors acknowledge financial support from the National Science Foundation of China under grant No. 61871081, National Key Research and Development Plan (Grant No. 2016YFA0300801, 2017YFB0406400). L.W.M. acknowledges support from the National Science Foundation under grant DMR-1708615.

ORCID

Yulong Liao https://orcid.org/0000-0003-1427-0717

Feiming Bai https://orcid.org/0000-0002-9431-4013

REFERENCES

1. Green MA, Bremner SP. Energy conversion approaches and materials for high-efficiency photovoltaics. Nat Mater. 2016;16:23–34.
2. Spanier JE, Fridkin VM, Rappe AM, Akbashev AR, Polemi A, Qi Y, et al. Power conversion efficiency exceeding the Shockley-Queisser limit in a ferroelectric insulator. Nat Photon. 2016;10:611–7.
3. Alexe M, Hesse D. Tip-enhanced photovoltaic effects in bismuth ferrite. Nat Commun. 2011;2:256.
4. Yang SY, Seidel J, Byrnes SJ, Shafer P, Yang C-H, Rossell MD, et al. Above-bandgap voltages from ferroelectric photovoltaic devices. Nat Nanotech. 2010;5:143–7.
5. Bhatnagar A, Chaudhuri AR, Kim YH, Hesse D, Alexe M. Role of domain walls in the abnormal photovoltaic effect in $BiFeO_3$. Nat Commun. 2013;4:2835.
6. Liu H, Chen J, Ren Y, Zhang L, Pan Z, Fan L, et al. Large Photovoltage and Controllable Photovoltaic Effect in PbTiO3-Bi(Ni2/3+xNb1/3-x)O3-δ Ferroelectrics. Adv Electron Mater. 2015; 1:1400051.
7. Choi T, Lee S, Choi YJ, Kiryukhin V, Cheong SW. Switchable ferroelectric diode and photovoltaic effect in BiFeO3. Science. 2009; 324:63-6.
8. Katiyar RK, Misra P, Mendoza F, Morell G, Katiyar RS. Switchable photovoltaic effect in bilayer graphene/$BiFeO_3$/Pt heterostructures. Appl Phys Lett. 2014;105:142902.
9. Guo R, You L, Chen L, Wu D, Wang JL. Photovoltaic property of $BiFeO_3$ thin films with 109° domains. Appl Phys Lett. 2011;99:122902.
10. Grinberg I, West DV, Torres M, Gou GY, Stein DM, Wu LY, et al. Perovskite oxides for visible-light-absorbing ferroelectric and photovoltaic materials. Nature. 2013; 503:509-12
11. Choi WS, Chisholm MF, Singh DJ, Choi T, Jellison GE Jr, Lee HN. Wide bandgap tunability in complex transition metal oxides by site-specific substitution. Nat Commun. 2012;3:689.
12. Zhang GH, Wu H, Li GB, Huang QZ, Yang CY, Huang FQ, et al. New high Tc multiferroics $KBiFe_2O_5$ with narrow band gap and promising photovoltaic effect. Sci Rep. 2013;3:1265.
13. Baettig P, Spaldin NA. Ab initio prediction of a multiferroic with large polarization and magnetization. Appl Phys Lett. 2005;86:012505.
14. Song ZW, Liu BG. Electronic structure and magnetic and optical properties of double perovskite Bi_2FeCrO_6 from first-principles investigation. Chinese Phys B. 2013; 22:047506.
15. Suchomel MR, Thomas CI, Allix M, Rosseinsky MJ, Fogg AM, Thomas MF. High pressure bulk synthesis and characterization of the predicted multiferroic $Bi(Fe_{1/2}Cr_{1/2})O_3$. Appl Phys Lett. 2007;90:112909.
16. Ichikawa N, Arai M, Imai Y, Hagiwara K, Sakama H, Azuma M, et al. Multiferroism at Room Temperature in $BiFeO_3$/$BiCrO_3$(111) Artificial Superlattices. Appl Phys Express. 2008;1:101302.
17. Khare A, Singh A, Prabhu SS, Rana DS. Controlling magnetism of multiferroic $(Bi_{0.9}La_{0.1})_2FeCrO_6$ thin films by epitaxial and crystallographic orientation strain. Appl Phys Lett. 2013;102:192911.
18. Nechache R, Rosei F. Recent progress in nanostructured multiferroic Bi_2FeCrO_6 thin films. J Solid State Chem. 2012;189:13–20.
19. Nechache R, Harnagea C, Li S, Cardenas L, Huang W, Chakrabartty J, et al. Bandgap tuning of multiferroic oxide solar cells. Nat Photon. 2014;9:61–7.
20. Quattropani A, Stoeffler D, Fix T, Schmerber G, Lenertz M, Versini G, et al. Band-gap tuning in ferroelectric Bi_2FeCrO_6 double perovskite thin films. J Phys Chem C. 2018;122:1070–7.
21. Shabadi V, Major M, Komissinskiy P, Vafaee M, Radetinac A, Yazdi MB, et al. Origin of superstructures in (double) perovskite thin films. J Appl Phys. 2014;116:114901.
22. Ohtomo A, Chakraverty S, Mashiko H, Oshima T, Kawasaki M. Spontaneous atomic ordering and magnetism in epitaxially stabilized double perovskites. J Mater Res. 2013;28:689–95.
23. Bai FM, Shi L, Zhang HW, Zhong ZY, Wang WD, He DW. Multiferroic properties of La-doped Bi2FeCrO6 prepared by high-pressure synthesis. J Appl Phys. 2012;111:07C702.
24. Rao CNR, Gopalakrishnan J, Vidyasagar K. Superstructures, Ordered Defects & Nonstoichiometry in Metal Oxides of Perovskite & Related Structures. Solid State Chemistry: Selected Papers of CNR Rao. 1995; 275-294.
25. Chen J, Chan HM, Harmer MP. Ordering structure and dielectric properties of undoped and La/Na-doped $Pb(Mg_{1/3}Nb_{2/3})O_3$. J Am Ceram Soc. 1989;72:593–8.
26. Baettig P, Ederer C, Spaldin NA. First principles study of the multiferroics $BiFeO_3$, Bi_2FeCrO_6, and $BiCrO_3$: Structure, polarization, and magnetic ordering temperature. Phys Rev B. 2005;72:214105.
27. Goffinet M, Íñiguez J, Ghosez P. First-principles study of a pressure-induced spin transition in multiferroic Bi_2FeCrO_6. Phys Rev B. 2012;86:024415.
28. Liu ZQ, Leusink DP, Wang X, Lü WM, Gopinadhan K, Annadi A, et al Metal-insulator transition in SrTiO3− x thin films induced by frozen-out carriers. Phys Rev lett. 2011;107:146802.
29. Liu ZQ, Lu W, Zeng SW, Deng JW, Huang Z, Li CJ, et al. Bandgap control of the oxygen-vacancy-induced two-dimensional electron gas in $SrTiO_3$. Adv Mater Interfaces. 2014;1:1400155.
30. Nechache R, Huang W, Li S, Rosei F. Photovoltaic properties of Bi_2FeCrO_6 films epitaxially grown on (100)-oriented silicon substrates. Nanoscale. 2016;8:3237–43.

31. Sun L, Fang YW, He J, Zhang YY, Qi RJ, He Q, et al. The preparation, and structural and multiferroic properties of B-site ordered double-perovskite Bi_2FeMnO_6. J Mater Chem C. 2017;5:5494.
32. Zhang JX, He Q, Trassin M, Luo W, Yi D, Rossell MD, et al. Microscopic origin of the giant ferroelectric polarization in tetragonal-like $BiFeO_3$. Phys Rev Lett. 2011;107:147602.
33. Zhang SR, Zhu YL, Tang YL, Liu Y, Li S, Han MJ, et al. Giant polarization sustainability in ultrathin ferroelectric films stabilized by charge transfer. Adv Mater. 2017;29:1703543.
34. Zhang LX, Chen J, Fan LL, Diéguez O, Cao JL, Pan Z, et al. Giant polarization in super-tetragonal thin films through interphase strain. Science. 2018;361:494–7.
35. Wang JL, Neaton JB, Zheng H, Nagarajan V, Ogale SB, Liu B, et al. Epitaxial $BiFeO_3$ multiferroic thin film heterostructures. Science. 2003;299:1719–22.
36. Shelke V, Mazumdar D, Srinivasan G, Kumar A, Jesse S, Kalinin S, et al. Reduced coercive field in $BiFeO_3$ thin films through domain engineering. Adv Mater. 2011;23:669–72.
37. Chu YH, Cruz MP, Yang CH, Martin LW, Yang PL, Zhang JX, et al. Domain control in multiferroic $BiFeO_3$ through substrate vicinality. Adv Mater. 2007;19:2662–6.

SUPPORTING INFORMATION

Additional supporting information may be found online in the Supporting Information section at the end of the article.

How to cite this article: Meng D, Xiao Y, He H, et al. Enhanced spontaneous polarization in double perovskite Bi_2FeCrO_6 films. *J Am Ceram Soc*. 2019;102:5234–5242. https://doi.org/10.1111/jace.16386